PERGAMON International Journal of Engineering Science 40 (2002) 1553–1577

International Journal of Engineering Science

www.elsevier.com/locate/ijengsci

A phenomenological multi-axial constitutive law for switching in polycrystalline ferroelectric ceramics

Robert M. McMeeking [a,*], Chad M. Landis [b]

[a] *Department of Mechanical and Environmental Engineering, University of California, Santa Barbara, CA 93106, USA*
[b] *Department of Mechanical Engineering and Materials Science, MS 321, Rice University, P.O. Box 1892, Houston, TX 77251, USA*

Received 7 January 2002; accepted 30 January 2002

Abstract

A phenomenological constitutive law for ferroelectric switching due to multi-axial mechanical and electrical loading of a polycrystalline material is developed. The framework of the law is based on kinematic hardening plasticity theory and has a switching surface in the space of mechanical stress and electric field that determines when non-linear response is possible. The size and shape of the switching surface in a modified electric field space remains fixed during non-linear behavior but its center moves around and thus is controlled by a kinematical hardening process. In general, the remanent polarization and the remanent strain are used as the internal variables that control how the center of the switching surface moves. However, the form presented in this paper has a one-to-one relationship between the remanent strain and the remanent polarization, simplifying the constitutive law and allowing remanent polarization to be used as the only internal variable controlling the kinematic effects. The constitutive law successfully reproduces hysteresis and butterfly loops for ferroelectric ceramics. The hysteresis and butterfly loops respond appropriately to the application of a fixed compressive stress parallel to the electric field. In addition, the law successfully handles remanent polarization rotation due to the application of electric field at an angle to the polarization direction.
© 2002 Elsevier Science Ltd. All rights reserved.

1. Introduction

Ferroelectrics are piezoelectrics in which the remanent electrical polarization $\boldsymbol{P}^{\mathrm{r}}$ can be altered by the application of an electric field [1]. In common ferroelectrics such as barium titanate and

* Corresponding author. Tel.: +1-805-893-4583; fax: +1-805-893-8486.
E-mail addresses: rmcm@engineering.ucsb.edu (R.M. McMeeking), landis@rice.edu (C.M. Landis).

0020-7225/02/$ - see front matter © 2002 Elsevier Science Ltd. All rights reserved.
PII: S0020-7225(02)00033-2

lead zirconate titanate (PZT), the polarization comes about due to the presence of ionic dipoles in the lattice. The polarization is the dipole moment per unit volume in the material and the remanent polarization is that remaining upon removal of the electric field and the mechanical stress. Alteration of the remanent polarization, called switching, takes place due to reorientation of the dipoles under the influence of the electric field. The existence of the dipoles is also associated with the presence of spontaneous strain at the lattice level. The reason for the strain is that the dipoles are formed when the cubic lattice distorts into a new symmetry such as tetragonal, rhombohedral or orthorhombic. Consequently, the remanently polarized state has a remanent strain $\boldsymbol{\varepsilon}^{\mathrm{r}}$ (equivalent to a plastic strain), where the remanent strain is the volume average of the lattice level spontaneous strain. The remanent strain alters during electrically driven switching and is also changed by application of mechanical stress in a non-dislocation plasticity process. Consequently, the remanent polarization can be modified by the application of stress. However, switching is limited in extent when the material has its dipoles and spontaneous strain aligned in the lattice as much as possible by a given electric field or mechanical stress and no further dipole reorientation is possible. If the electric field and/or the mechanical stress is kept in its given orientation in this situation and increased, no further switching will occur and the material is said to be in lock-up. However, as Huber and Fleck [2] have shown, polarization rotation is possible in this state when an electric field is applied at an angle to the current remanent polarization.

Ferroelectrics are used in piezoelectric form as sensors to convert acoustic and mechanical signals into electrical ones and as actuators to convert electrical impulses into motions [1]. In both of these applications and in others, somewhat complex shapes of polycrystalline ferroelectric material are utilized in conjunction with electrodes [3]. For design of these shapes, for simulation of device performance and for life prediction of components, non-linear constitutive laws are required that are capable of modeling switching in a reliable manner. It is the purpose of this paper to provide a relatively simple law that can simulate the non-linear switching behavior of polycrystalline ferroelectrics subject to multi-axial stress and an arbitrary electric field.

Several non-linear constitutive models have been developed for ferroelectric ceramics. In some of these, a microelectromechanical approach has been taken in which individual crystallites are identified and rules introduced to predict when each one will switch completely under the influence of applied stress and electric field [4,5]. Such models have been quite successful at predicting the homogeneous average response of polycrystalline material [3,6,7]. For accuracy, these models require many hundreds or thousands of crystallites. Consequently, when used as a constitutive law in calculations for heterogeneous response of the ferroelectric such as in finite element solutions, computations are slow and inefficient. Nevertheless, this approach or variants of it have been successfully used as constitutive laws in such calculations [3,8].

An improved constitutive law was developed by Huber et al. [9] who used domain wall motion as the basis of a microelectromechanical model. Domains are regions in which the spontaneous polarization and strain is homogeneous and are divided from each other within a single crystal by mobile walls. The resulting constitutive law, analogous to a polycrystalline slip model, is accurate and physically appealing since switching is known to occur gradually by domain wall motion. However, accuracy is still predicated upon the presence of many hundreds or thousands of grains each having many domains. Therefore, computation with this constitutive model is also slow. However, Huber and Fleck [2] have developed a version of this approach in which a reduced number of grains is used and calculation in this situation is rapid. They show that the reduced

system also retains a reasonable level of accuracy. A constitutive law in the same spirit as the reduced grain scheme of Huber and Fleck [2] is that of Chen et al. [10] who use the lowering of the Gibbs free energy as the driving force for domain switching. Chen et al. [10] formulate their model in terms of domain volume fractions for a single crystal but fit their results to the behavior of polycrystalline ferroelectrics.

Another class of constitutive models is phenomenological in which functions of electric field and mechanical stress are devised for predicting the corresponding electric displacement and strain. The functions are generally fitted to experimental data or are given elementary forms that plausibly reproduce the physical behavior. Perhaps the first such phenomenological model for ferroelectric switching was that of Chen and co-workers [11–14]. This dynamic model is capable of producing good hysteresis and butterfly loops in response to a cyclic electric field. Chen [13] developed a 3-dimensional version of the model but no results were presented for multi-axial electromechanical loadings. Even very recently, phenomenological constitutive laws with a microelectromechanical basis such as that of Zhou and Chattopadhyay [15] have been developed for which there is no obvious way to generalize them to complex multi-axial electromechanical loadings. Maugin and co-workers [16–19] were the first to develop a framework for phenomenological constitutive laws capable of handling complex multi-axial electromechanical loading. The framework has a thermodynamic basis utilizing the Helmholtz free energy and makes use of concepts of phenomenological plasticity theory including yield surfaces and isotropic and kinematic hardening. The polarization response of the material during initial poling is characterized and hysteresis loops during cyclic electrical loading are given. Although their framework is quite comprehensive, Maugin et al. [16–19] do not provide complete recipes for a constitutive model of any particular ferroelectric, nor do they demonstrate the prediction of butterfly loops. In addition, the response of their model to multi-axial electromechanical loading is not illustrated.

A rather complete phenomenological constitutive model for ferroelectric materials subject to switching has been developed by Kamlah and co-workers [20–26]. This constitutive law is based on a framework akin to that of Maugin et al. [16–19] and uses a number of non-linear functions to represent behavior during switching. The approach involves a number of logical rules for handling the different circumstances that arise in complex electromechanical loadings. Kamlah et al. [20–22] have used the method to produce reasonable hysteresis and butterfly loops for ferroelectrics and a 3-dimensional formulation is available [23]. Comparisons have been made successfully with polarization rotation behavior [25] and investigations of the effect of stress during hysteresis cycling have been made [26]. In addition, the constitutive law has been used in finite element calculations to predict the poling stresses in a stack actuator [24]. Thus, the constitutive law of Kamlah et al. [20–26] is attractive and effective; however, alternative approaches for developing phenomenological constitutive models are also feasible.

Another phenomenological approach based on the concepts of Maugin et al. [16–19] stems from the ideas of Cocks and McMeeking [27] who explicitly pursue the notion of a plastic yielding-like switching criterion and the use of kinematic hardening concepts to characterize the behavior of ferroelectrics. However, only a 1-dimensional model was presented in [27]. Later, McMeeking [28] modified the formulation somewhat and demonstrated how the concepts can be used to generate realistic hysteresis and butterfly loops plus give the correct qualitative response to complex electromechanical loading. However, Landis [29] has taken this framework and constructed a thermodynamically rigorous and complete 3-dimensional constitutive law that matches

all the available data for ferroelectric switching in the form of hysteresis and butterfly loops, stress–strain behavior, and combined electromechanical [30] and non-proportional electrical loading [2]. In order to obtain agreement with all of the diverse types of behaviors exhibited by ferroelectric ceramics, nine internal variables, corresponding to the components of remanent strain and remanent polarization, were employed in [29]. Furthermore, electromechanical coupling was needed in both the switching surface and the kinematic hardening potential in order to predict all of the observations. The purpose of the current paper is to present a simplified formulation of the approach in [29] that employs only three internal variables by rigidly linking the remanent strain to the remanent polarization. Hence, this link accounts for all non-linear electromechanical coupling in the formulation. Due to the one-to-one coupling between the remanent polarization and the remanent strain, the switching criterion can be phrased entirely in terms of a modified electric field variable. Furthermore, the kinematic hardening potential, which is used to derive hardening moduli, can be given as a function of only the remanent polarization. As expected, this simpler formulation comes at the expense of a more restricted versatility. However, we believe that the proposed formulation has some utility due to its relative simplicity, even though it would be incapable of reproducing some known phenomena in polycrystalline ferroelectrics.

2. Basic equations

In this section the equations governing small deformation, isothermal, ferroelectric behavior will be reviewed. Throughout, standard Einstein notation is utilized with summation implied over repeated indices. A comma followed by a subscript implies differentiation with respect to the coordinate with the same subscript.

Consider a volume of ferroelectric material, V, bounded by the surface, S. Gauss' law is stated as

$$D_{i,i} = q^v \quad \text{in} \quad V \tag{1}$$

and

$$[\![D_i]\!]\tilde{n}_i = q^s \quad \text{on} \quad S \tag{2}$$

where $\mathbf{D}$ is the electric displacement, q^v is the free charge per unit volume in V, q^s is the free charge per unit area on S, $\tilde{\mathbf{n}}$ is the unit normal to S pointing outwards from V and $[\![\ ]\!]$ denotes the jump across S of the quantity within, computed as the value outside V minus the value inside V. Mechanical equilibrium of stresses is given by

$$\sigma_{ij,i} = -b_j \quad \text{in} \quad V \tag{3}$$

and

$$[\![\sigma_{ij}]\!]\tilde{n}_j = -t_i \quad \text{on} \quad S \tag{4}$$

where $\boldsymbol{\sigma}$ is the stress, $\mathbf{b}$ is the body force per unit volume in V and $\mathbf{t}$ is the surface traction on S.

The electric field, **E**, is related to the gradient of the potential ϕ by

$$E_i = -\phi_{,i} \tag{5}$$

and the strain $\boldsymbol{\varepsilon}$ is related to the displacement **u** by

$$\varepsilon_{ij} = \tfrac{1}{2}(u_{i,j} + u_{j,i}) \tag{6}$$

The linear piezoelectric relationships are

$$D_i - P_i^{\mathrm{r}} = d_{ikl}\sigma_{kl} + \kappa_{ij}^{\sigma} E_j \tag{7}$$

$$\varepsilon_{ij} - \varepsilon_{ij}^{\mathrm{r}} = s_{ijkl}^{\mathrm{E}}\sigma_{kl} + d_{kij}E_k \tag{8}$$

where $\boldsymbol{P}^{\mathrm{r}}$ and $\boldsymbol{\varepsilon}^{\mathrm{r}}$ are the remanent polarization and strain, $\mathbf{s}^{\mathrm{E}}$ is the elastic compliance tensor at constant electric field, **d** is a tensor of piezoelectric coefficients, and $\boldsymbol{\kappa}^{\sigma}$ is the dielectric permittivity tensor at constant stress. For this work we will assume that $\mathbf{s}^{\mathrm{E}}$ and $\boldsymbol{\kappa}^{\sigma}$ are isotropic and **d** is transversely isotropic about the polarization direction such that

$$s_{ijkl}^{\mathrm{E}} = \frac{1+v}{2Y}(\delta_{ik}\delta_{jl} + \delta_{il}\delta_{jk}) - \frac{v}{Y}\delta_{ij}\delta_{kl} \tag{9}$$

$$\kappa_{ij}^{\sigma} = \kappa\delta_{ij} \tag{10}$$

$$d_{kij} = \frac{P^{\mathrm{r}}}{P_0}\left[d_{33}n_k n_i n_j + d_{31}n_k\alpha_{ij} + \frac{1}{2}d_{15}(n_i\alpha_{jk} + n_j\alpha_{ik})\right] \tag{11}$$

where Y is the Young's modulus, v is the Poisson's ratio, κ is the isotropic dielectric permittivity, $P^{\mathrm{r}} = [P_i^{\mathrm{r}}P_i^{\mathrm{r}}]^{1/2}$ is the magnitude of the remanent polarization, $\boldsymbol{n} = \boldsymbol{P}^{\mathrm{r}}/P^{\mathrm{r}}$ is the direction of the remanent polarization, δ_{ij} is the Kronecker delta, $\alpha_{ij} = \delta_{ij} - n_i n_j$, P_0 is the maximum attainable remanent polarization magnitude, and d_{33}, d_{31} and d_{15} are the longitudinal, transverse and shear piezoelectric constants when the ceramic is completely poled. Furthermore, we will assume that $d_{15} = d_{33} - d_{31}$. This relationship will greatly simplify the model and is actually a reasonable assumption. Coincidentally, the piezoelectric coefficients reported for poled polycrystalline $BaTiO_3$ [31] exactly satisfy this relation. Note that the assumption that the elasticity and the dielectric permittivity tensors are isotropic and constant ignores the effect of polarization texture on the response of the ceramic. This effect is known to be small in many materials [1].

3. Constitutive framework

The constitutive law will be developed for a polycrystalline material under isothermal conditions. Cocks and McMeeking [27] and Landis [29] have proposed constitutive laws similar to that which will be described. However, the one presented by Cocks and McMeeking [27] is somewhat rudimentary and serves only to illustrate concepts developed for the constitutive framework. In

addition, only 1-dimensional examples were presented and a 3-dimensional generalization was not developed. The formulation given by Landis [29] is essentially complete and convincing. On the other hand, there are alternative approaches compared to Landis' [29] that are available and with the added advantage that a simpler structure can be achieved. It is the purpose of this paper to present an alternative formulation that is a considerable simplification compared with Landis' [29] constitutive law and those of others, but keeping within the same thermodynamic framework. The primary assumption that we will use to achieve this simplification is that the remanent strain in the material is directly linked to the remanent polarization such that

$$\varepsilon^{\mathrm{r}}_{ij} = \frac{\varepsilon_0}{2P_0^2}\left(3P^{\mathrm{r}}_i P^{\mathrm{r}}_j - \delta_{ij}P^{\mathrm{r}}_k P^{\mathrm{r}}_k\right) \tag{12}$$

where ε_0 is the remanent strain corresponding to the maximum achievable remanent polarization P_0. Hence, the reader should note that the remanent strain could be replaced by the remanent polarization, via Eq. (12), in any of the following equations. However, the apparent dependence on $\boldsymbol{\varepsilon}^{\mathrm{r}}$ will be maintained in order to keep the equations simple and understandable. The result in Eq. (12) states that there is an incompressible elongation of the material parallel to the remanent polarization. A quadratic relationship between the polarization and the strain is used in Eq. (12) because this is commonly assumed to be the case [1]. Other relationships such as a linear dependence on the absolute value of the remanent polarization are possible and we do not mean to preclude other choices. However, the presentation will be clearest when a specific form as in Eq. (12) is used. In addition, the results we obtain with Eq. (12) are quite reasonable, so it seems to be an acceptable choice.

The main objection to connecting the remanent strain uniquely to the remanent polarization as in Eq. (12) is that some experimental results contradict this. For example, applying stress to an unpoled sample causes remanent strain without remanent polarization. In addition, there are other experimental results where the remanent strain does not have a one-to-one relationship with the remanent polarization [30]. Furthermore, Eq. (12) does not allow for compressive remanent strains parallel to the remanent polarization. Our approach is to recognize that there are deficiencies with this assumption, but to assert that Eq. (12) is a reasonable approximation when electric fields are strong and stresses are small.

With Eq. (12) and following Bassiouny et al. [16–19], Cocks and McMeeking [27], and Landis [29], a Helmholtz free energy for the material is introduced as

$$\Psi = \Psi^{\mathrm{s}}(\boldsymbol{\varepsilon}, \mathbf{D}, \boldsymbol{P}^{\mathrm{r}}) + \Psi^{\mathrm{r}}(\boldsymbol{P}^{\mathrm{r}}) \tag{13}$$

where Ψ^{s} is the reversibly stored part of the free energy and Ψ^{r} depends on changes in the remanent state of the material. This form differs from [16–19,27,29] in that it does not contain an explicit dependence on the remanent strain. The reversibly stored free energy is written as

$$\Psi^{\mathrm{s}} = \tfrac{1}{2}c^D_{ijkl}(\varepsilon_{ij} - \varepsilon^{\mathrm{r}}_{ij})(\varepsilon_{kl} - \varepsilon^{\mathrm{r}}_{kl}) - h_{kij}(D_k - P^{\mathrm{r}}_k)(\varepsilon_{ij} - \varepsilon^{\mathrm{r}}_{ij}) + \tfrac{1}{2}\beta^{\varepsilon}_{ij}(D_i - P^{\mathrm{r}}_i)(D_j - P^{\mathrm{r}}_j) \tag{14}$$

where $\mathbf{c}^{\mathrm{D}}$ is the elastic stiffness tensor at constant electric displacement, $\mathbf{h}$ is a tensor of piezoelectric coefficients and $\boldsymbol{\beta}^{\varepsilon}$ is the inverse dielectric permittivity tensor at constant strain. The

tensors $\mathbf{c}^{\mathrm{D}}$, $\mathbf{h}$ and $\boldsymbol{\beta}^{\varepsilon}$ are algebraically related to $\mathbf{s}^{\mathrm{E}}$, $\mathbf{d}$ and $\boldsymbol{\kappa}^{\sigma}$. The stress and electric field are derived from the Helmholtz free energy as

$$E_i = \frac{\partial \Psi}{\partial D_i} = \frac{\partial \Psi^{\mathrm{s}}}{\partial D_i} = -h_{ijk}(\varepsilon_{jk} - \varepsilon^{\mathrm{r}}_{jk}) + \beta^{\varepsilon}_{ij}(D_j - P^{\mathrm{r}}_j) \tag{15}$$

and

$$\sigma_{ij} = \frac{\partial \Psi}{\partial \varepsilon_{ij}} = \frac{\partial \Psi^{\mathrm{s}}}{\partial \varepsilon_{ij}} = c^{\mathrm{D}}_{ijkl}(\varepsilon_{kl} - \varepsilon^{\mathrm{r}}_{kl}) - h_{kij}(D_k - P^{\mathrm{r}}_k) \tag{16}$$

The dissipation $\dot{\Delta}$ is the external rate of work done on the material less the rate at which work is stored in the Helmholtz free energy. By differentiating Eq. (13), applying a Legendre transformation to determine simplified forms for the derivatives of Eq. (14), implementing Eqs. (15) and (16), and using the derivatives of (11) and (12), one can show that the dissipation rate is given as

$$\dot{\Delta} = \sigma_{ij}\dot{\varepsilon}_{ij} + E_i\dot{D}_i - \dot{\Psi} = \widehat{E}_i\dot{P}^{\mathrm{r}}_i \tag{17}$$

where

$$\widehat{E}_i = E_i + \frac{3\varepsilon_0}{P_0^2}s_{ij}P^{\mathrm{r}}_j + \frac{\partial d_{qrs}}{\partial P^{\mathrm{r}}_i}E_q\sigma_{rs} - E^{\mathrm{B}}_i \tag{18}$$

with the deviatoric part of the stress $s_{ij} = \sigma_{ij} - \delta_{ij}\sigma_{kk}/3$, and the back electric field, $\mathbf{E}^{\mathrm{B}}$, defined as

$$E^{\mathrm{B}}_i = \frac{\partial \Psi^{\mathrm{r}}}{\partial P^{\mathrm{r}}_i}. \tag{19}$$

The derivatives of the piezoelectric tensor appearing in the third term on the right hand side of Eq. (18) have been given by Landis [29], and for completeness they are listed again here as

$$\begin{aligned}\frac{\partial d_{kij}}{\partial P^{\mathrm{r}}_l} &= \frac{d_{33}}{P_0}(n_k n_i n_j n_l + n_i n_j \alpha_{kl} + n_k n_j \alpha_{il} + n_k n_i \alpha_{jl}) \\ &\quad + \frac{d_{31}}{P_0}(\alpha_{ij}\alpha_{kl} + n_k n_l \alpha_{ij} - n_i n_k \alpha_{jl} - n_j n_k \alpha_{il}) \\ &\quad + \frac{d_{15}}{2P_0}(\alpha_{il}\alpha_{jk} + \alpha_{ik}\alpha_{jl} + n_i n_l \alpha_{jk} + n_j n_l \alpha_{ik} - n_i n_k \alpha_{jl} - n_j n_k \alpha_{il} - 2n_i n_j \alpha_{kl})\end{aligned} \tag{20}$$

As Landis [29] has noted, the dissipation rate is guaranteed to be non-negative and the postulate of maximum dissipation will be satisfied if an associated flow rule is used with the switching criterion

$$\Phi(\widehat{\mathbf{E}}, \boldsymbol{P}^{\mathrm{r}}) = \mathbf{0}. \tag{21}$$

Furthermore, Φ must be convex in $\widehat{\mathbf{E}}$ space, and enclose the location $\widehat{\mathbf{E}} = \mathbf{0}$. Note that the convex switching surface along with the associated flow rule does not necessarily imply material stability,

only maximum remanent/plastic dissipation. During switching, the associated flow rule implies that the increment of remanent polarization must be normal to the switching surface such that

$$\dot{P}_i^{\mathrm{r}} = \lambda \frac{\partial \Phi}{\partial \widehat{E}_i} = \lambda \widehat{P}_i \tag{22}$$

where λ is a positive scalar multiplier to be determined, and $\widehat{\boldsymbol{P}}$ is defined in Eq. (22). If $\Phi < 0$, linear response occurs without any switching, whereas $\Phi > 0$ is forbidden. Thus, Φ is a switching surface, analogous to a yield surface in plasticity [16–19,27–29,32].

During switching the consistency condition must be satisfied, i.e. $\dot{\Phi} = 0$. Along with the following definitions,

$$\widehat{P}_i = \widehat{P}_i + \frac{\partial d_{ikl}}{\partial P_j^{\mathrm{r}}} \sigma_{kl} \widehat{P}_j \tag{23}$$

$$\hat{\varepsilon}_{ij} = \frac{\partial d_{kij}}{\partial P_l^{\mathrm{r}}} E_k \widehat{P}_l + \frac{3\varepsilon_0}{2P_0^2} \left(P_i^{\mathrm{r}} \widehat{P}_j + P_j^{\mathrm{r}} \widehat{P}_i - \frac{2}{3} P_k^{\mathrm{r}} \widehat{P}_k \delta_{ij} \right) \tag{24}$$

and

$$\mathscr{D} = \left(H_{ij} - \frac{3\varepsilon_0}{P_0^2} s_{ij} \right) \widehat{P}_i \widehat{P}_j - \frac{\partial \Phi}{\partial P_i^{\mathrm{r}}} \widehat{P}_i \tag{25}$$

where the hardening moduli are

$$H_{ij} = \frac{\partial E_i^{\mathrm{B}}}{\partial P_j^{\mathrm{r}}} = \frac{\partial \Psi^{\mathrm{r}}}{\partial P_i^{\mathrm{r}} \partial P_j^{\mathrm{r}}} \tag{26}$$

the consistency condition yields an equation for the plastic multiplier, λ, with the solution

$$\lambda = \frac{1}{\mathscr{D}} (\widehat{P}_i \dot{E}_i + \hat{\varepsilon}_{ij} \dot{\sigma}_{ij}) \tag{27}$$

Note that another term involving second derivatives of the piezoelectric tensor with respect to the remanent polarization would have appeared in the expression for $\mathscr{D}$ if we had not used the assumption that $d_{15} = d_{33} - d_{31}$.

Now, (22) and (27) can be used to determine the remanent polarization increment, (12) can be used to determine the remanent strain increment, and during switching the incremental forms of (7) and (8) can be shown to be

$$\dot{D}_i = \left(d_{ikl} + \frac{1}{\mathscr{D}} \widehat{P}_i \hat{\varepsilon}_{kl} \right) \dot{\sigma}_{kl} + \left(\kappa_{ij}^{\sigma} + \frac{1}{\mathscr{D}} \widehat{P}_i \widehat{P}_j \right) \dot{E}_j \tag{28}$$

$$\dot{\varepsilon}_{ij} = \left(s_{ijkl}^{\mathrm{E}} + \frac{1}{\mathscr{D}} \hat{\varepsilon}_{ij} \hat{\varepsilon}_{kl} \right) \dot{\sigma}_{kl} + \left(d_{kij} + \frac{1}{\mathscr{D}} \widehat{P}_k \hat{\varepsilon}_{ij} \right) \dot{E}_k \tag{29}$$

Note that as in [29], the tangent moduli are symmetric.

4. Proposed switching surface and hardening moduli

The simplest choice for the switching surface that meets the convexity requirement is

$$\Phi = \widehat{E}_i \widehat{E}_i - E_0^2 \tag{30}$$

where E_0 is the coercive field, i.e. the critical field to cause switching. Note that we will consider the coercive field to be constant and therefore the shape of the function Φ is a sphere in $\mathbf{E}$ space of fixed radius E_0. There are other possibilities such as taking the coercive field to vary, in particular to increase as switching occurs, thereby introducing a degree of isotropic hardening into the switching criterion. In this paper we will confine ourselves to purely kinematic hardening with a fixed value for E_0 although there is evidence that some isotropic hardening occurs during the poling stage of the material response [33]. We will find that purely kinematic hardening gives satisfactory hysteresis and butterfly loops. Another point is that according to Eq. (30), the shape of Φ remains fixed during switching. This is again the simplest choice, since the switching surface could easily change shape during non-linear behavior. However, we will find that the results we obtain with Eq. (30) are reasonably satisfactory. We also note similarities of this switching surface to those used in [29]. In a model proposed for fine grained $BaTiO_3$, remanent strains were not allowed, and hence the internal variables of the model were the components of the remanent polarization. For that material, a similar switching surface to Eq. (30) was proposed in a different modified electric field space. Landis [29] also extended the model in an attempt to describe materials with full electromechanical coupling. If we expand Eq. (30) into standard stress and electric field space, we find that the invariants, $E_i E_i$, $E_i s_{ij} P_j^{\mathrm{r}}$, and $s_{ik} s_{ij} P_j^{\mathrm{r}} P_k^{\mathrm{r}}$, are used to describe the switching surface. This is compared to $E_i E_i$, $E_i s_{ij} P_j^{\mathrm{r}}$, and $s_{ij} s_{ij}$ in [29] for the coupled electromechanical case. Since the remanent strain is rigidly coupled to the remanent polarization, $s_{ij} s_{ij}$ cannot appear in this simplified model. However, this model suggests the invariant $s_{ik} s_{ij} P_j^{\mathrm{r}} P_k^{\mathrm{r}}$, which may be able to improve the more general formulation.

The criterion for switching given by $\Phi = 0$ inserted into Eq. (30) appears to be reasonably sensible. When the electric field is aligned with an existing remanent polarization, a tensile stress enhances the tendency for the polarization to increase and a compressive stress limits it. When the electric field opposes an existing remanent polarization, the stress has the opposite effect. In addition, the kinematic nature of the hardening in the switching condition $\Phi = 0$ with Φ given by Eq. (30) is clear. If the stress is assumed to be zero, it can then be seen that the switching surface is a sphere of constant radius E_0 in the space of electric field, centered at $\mathbf{E}^{\mathrm{B}}$. However, $\mathbf{E}^{\mathrm{B}}$ is a function of the remanent polarization, so as switching causes the backfield to change, the spherical surface moves around in electric field space, causing changes to the electric field required to drive switching. When the stress is non-zero, the switching surface can still be thought of as a sphere of constant radius in the space of electric field centered at $\mathbf{E}^{\mathrm{B}}$ but the electric field is augmented by an amount determined by the stress and the remanent polarization. However, the switching surface still moves around in response to changes in remanent polarization, so kinematic hardening effects occur in the presence of combined electromechanical loading as well as when electric field alone is applied.

What remains to complete the model is the specification of the remanent potential Ψ^{r}. In an initially isotropic material, the function Ψ^{r} can depend only on the magnitude P^{r} of the vector $\boldsymbol{P}^{\mathrm{r}}$. In these circumstances, the back electric field is given by

$$E_i^{\mathrm{B}} = \frac{\partial \Psi^{\mathrm{r}}}{\partial P_i^{\mathrm{r}}} = \frac{\mathrm{d}\Psi^{\mathrm{r}}}{\mathrm{d}P^{\mathrm{r}}} n_i \tag{31}$$

where again **n** is the unit vector parallel to the remanent polarization. Thus, the back electric field is parallel to the remanent polarization and it resists the switching impetus of the electric field and the stress exactly in the direction opposite to the remanent polarization. Clearly, the magnitude of the back electric field, E^{B}, is

$$E^{\mathrm{B}} = \frac{\mathrm{d}\Psi^{\mathrm{r}}}{\mathrm{d}P^{\mathrm{r}}} \tag{32}$$

Differentiation of the back electric field with respect to the remanent polarization then gives

$$H_{ij} = \frac{\partial^2 \Psi^{\mathrm{r}}}{\partial P_i^{\mathrm{r}} \partial P_j^{\mathrm{r}}} = \frac{\mathrm{d}^2 \Psi^{\mathrm{r}}}{\mathrm{d}(P^{\mathrm{r}})^2} n_i n_j + \frac{\mathrm{d}\Psi^{\mathrm{r}}}{\mathrm{d}P^{\mathrm{r}}} \frac{1}{P^{\mathrm{r}}} (\delta_{ij} - n_i n_j) \tag{33}$$

Calibration of the constitutive law is most readily achieved by fitting it to a portion of a hysteresis loop. For this purpose, the 1-dimensional version of the law is required with the remanent polarization and the electric field parallel to each other. For later reference, the stress will be retained in the 1-dimensional version but restricted to being coaxial with the electric field. In these circumstances the switching criterion Eq. (21), subject to Eq. (30), becomes

$$E + \frac{2\varepsilon_0}{P_0^2} \sigma P^{\mathrm{r}} n + \frac{d_{33}}{P_0} \sigma E - E^{\mathrm{B}} n = \pm E_0 \tag{34}$$

and otherwise the magnitude of the left hand side must be less than E_0. In Eq. (34), E is the axial electric field, σ is the stress, P^{r} is the remanent polarization magnitude, n is the remanent polarization direction, i.e. $n = \pm 1$, and E^{B} is the back electric field magnitude. All quantities are parallel to the electric field and E and σ in Eq. (31) are signed, i.e. they are not magnitudes, while P^{r} and E^{B} are always positive. Similarly, Eq. (22) becomes

$$\dot{P}^{\mathrm{r}} = \frac{\dot{E} + \frac{2\varepsilon_0}{P_0^2} \dot{\sigma} P^{\mathrm{r}} n}{\frac{\mathrm{d}^2 \Psi^{\mathrm{r}}}{\mathrm{d}(P^{\mathrm{r}})^2} - \frac{2\varepsilon_0}{P_0^2} \sigma} \tag{35}$$

In the absence of stress, Eq. (34) becomes

$$E - E^{\mathrm{B}} n = \pm E_0 \tag{36}$$

and Eq. (35) is

$$\dot{P}^{\mathrm{r}} = \frac{\dot{E}}{\dfrac{\mathrm{d}^2\Psi^{\mathrm{r}}}{\mathrm{d}(P^{\mathrm{r}})^2}} \tag{37}$$

This equation can be integrated to give

$$\frac{\mathrm{d}\Psi^{\mathrm{r}}}{\mathrm{d}P^{\mathrm{r}}} = E^{\mathrm{B}}(P^{\mathrm{r}}) = |E(P^{\mathrm{r}})| - E_0 \tag{38}$$

where Eq. (36) has been used to establish the constant of integration and $|E|$ is the magnitude of the electric field. Note that Eqs. (36) and (38) are essentially identical. However, Eq. (38) indicates how calibration is carried out. The coercive field is the half width of the hysteresis loop at zero remanent polarization. Then with the magnitude of the electric field from a half cycle of the hysteresis loop plotted against the magnitude of the remanent polarization, the function Ψ^{r} (or alternatively the function E^{B}) can be fitted to the results.

5. Results

The constitutive law will now be illustrated through examples of hysteresis and butterfly loops and stress–strain curves. Instead of fitting the law to materials data, we will use a functional form for Ψ^{r} that produces plausible shapes for the loops and stress–strain curves. Following Huber and Fleck [2], the function we will use is

$$\Psi^{\mathrm{r}} = -HP_0^2\left[\ln\left(1-\frac{P^{\mathrm{r}}}{P_0}\right)+\frac{P^{\mathrm{r}}}{P_0}\right] \tag{39}$$

where H is a constant. Thus Eq. (32) provides

$$E^{\mathrm{B}} = \frac{HP^{\mathrm{r}}}{1-\frac{P^{\mathrm{r}}}{P_0}} \tag{40}$$

which means that the magnitude of the effective back field diverges as P^{r} approaches P_0 from below. As the effective back field diverges, the magnitude of the electric field from Eq. (36) necessary to drive switching increases without limit. As a consequence, large increases of electric field are associated with very small increases of remanent polarization as P^{r} approaches P_0 and the applied electric field eventually diverges in the limit. This has the effect of ensuring that P^{r} cannot exceed P_0 and therefore the remanent polarization process locks up upon approaching this limiting value.

Subject to Eq. (40), Eq. (36) is used to obtain the hysteresis loop shown in Fig. 1 for an initially unpolarized material. For this loop, the plot is started at zero electric field, zero electric displacement and zero remanent polarization. Since the electric field E is initially lower than the

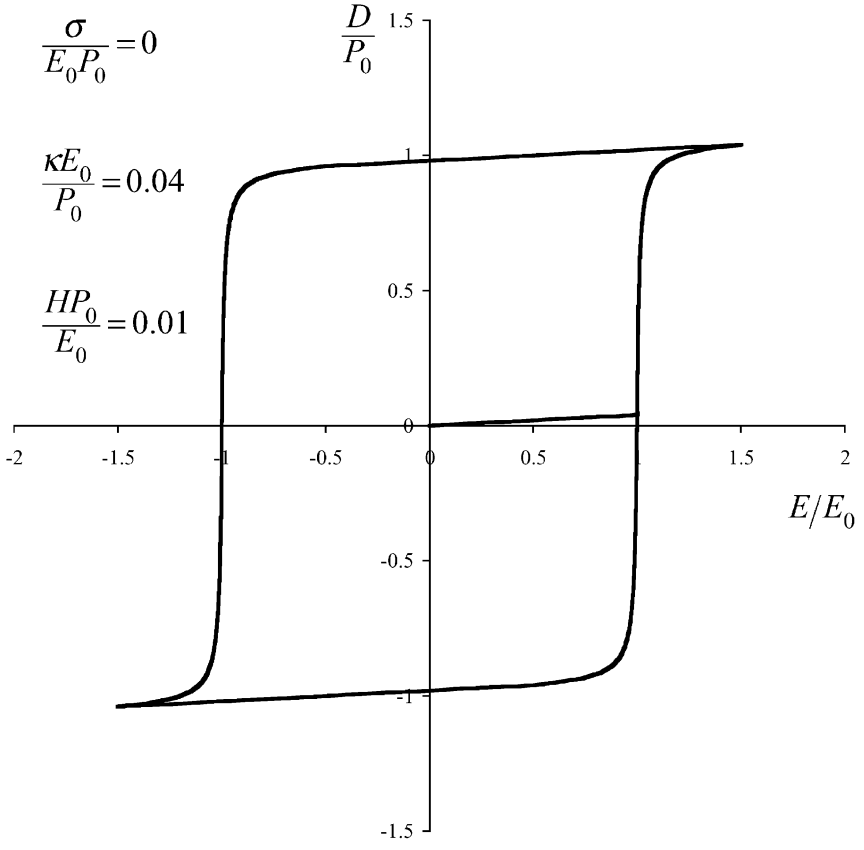

Fig. 1. Hysteresis loop obtained using the constitutive law.

coercive field E_0, the response is initially linear as E is increased with the remanent polarization remaining zero. In the initial response starting at the origin in Fig. 1, the behavior is given by

$$D = \kappa E \tag{41}$$

where D is the electric displacement parallel to the electric field. When the electric field reaches the coercive value, E_0, switching begins to occur and then Eq. (40) is used along with Eq. (36) with the positive sign in the right hand side to compute the response. To convert the remanent polarization to the electric displacement, the relationship

$$D = \kappa E + P^{\mathrm{r}} n \tag{42}$$

is utilized. Initially there is a steep slope indicating that large amounts of polarization are taking place with only small increases in the electric field. Correspondingly, the back electric field, E^{B}, remains small. However, as P^{r} approaches P_0, the back field begins to grow rapidly and as a result the electric field required to drive switching begins to increase rapidly even for relatively small increases of the remanent polarization. The electrical polarization process locks up and the slope

of the hysteresis loop approaches κ as the electric field increases. It should be emphasized that the observed effect arises because of the kinematic hardening embedded in the constitutive law. During this lock up process, the switching surface translates along the positive electric field axis. The center of the switching surface (i.e. the back field) starts at the origin and follows a curve parallel to the segment of the hysteresis loop corresponding to switching.

In the example shown in Fig. 1, the electric field is increased until it equals $1.5E_0$ and then it is reversed. Reduction of the electric field at this stage causes Φ to fall below zero, so that linear response sets in once more but now according to Eq. (42) with P^{r} non-zero and held fixed. This continues until the electric field falls to $-0.5E_0$ at which value Φ once more equals zero. Thus switching recommences and Eq. (36) is used once more but now with the negative sign in the right hand side. The switching is now such that the remanent polarization shrinks. The back field continues to be given by Eq. (40) and its magnitude diminishes until it disappears when the remanent polarization is zero and the E is equal to $-E_0$. Thereafter the remanent polarization and the back field both become negative but their magnitudes are still related by Eq. (40). Thus the center of the switching surface (i.e. the back field) retraces the path it followed while the remanent polarization was increasing, moves through the origin and then to its left, always following a path parallel to the hysteresis loop.

The electric field is reduced to $-1.5E_0$ and then increased. Upon this reversal, Φ once more falls below zero and linear response following Eq. (42) occurs with P^{r} fixed. This continues until $E = 0.5E_0$ when Φ returns to zero and switching now recommences, causing P^{r} to increase. For this portion of the curve, Eq. (36) is used with the positive sign in the right hand side and Eq. (40) relates the magnitude of the back field to the magnitude of the remanent polarization. The response is such that the right side of the hysteresis curve is parallel to the left side. The cycle is complete when the remanent polarization and the back field disappear and E is once more equal to E_0. Continued cycling of the electric field between the limits $-1.5E_0$ and $1.5E_0$ produces repetitions of the initial loop.

The loop shown in Fig. 1, and all subsequent loops, are obtained using $\kappa E_0/P_0 = 0.04$ and $HP_0E_0 = 0.01$ as noted on the figure. These values are chosen simply because they produce a shape for the hysteresis loop that compares well with experimental ones [1,30].

A butterfly loop is computed corresponding to the hysteresis loop shown in Fig. 1 and is shown in Fig. 2. For a material with a fixed isotropic elasticity tensor, the axial strain ε is computed from Eq. (8) as

$$\varepsilon = \frac{\sigma}{Y} + \frac{P^{\mathrm{r}} n}{P_0} d_{33} E + \varepsilon^{\mathrm{r}} \tag{43}$$

where Y is a constant Young's modulus and ε^{r} is the axial remanent strain. The remanent strain is computed from Eq. (12) as

$$\varepsilon^{\mathrm{r}} = \varepsilon_0 \left(\frac{P^{\mathrm{r}}}{P_0} \right)^2 \tag{44}$$

With Eqs. (43) and (44) available, the butterfly loop shown in Fig. 2 is computed directly from the results illustrated in Fig. 1, with the stress, σ, equal to zero. The piezoelectric response is

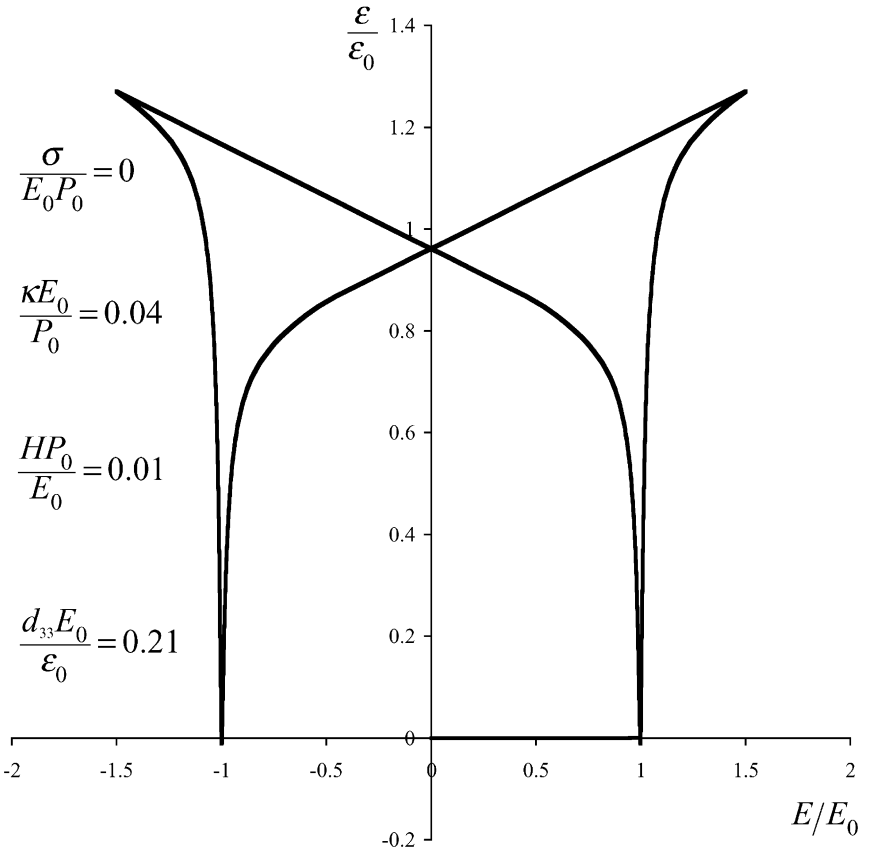

Fig. 2. Butterfly loop corresponding to the hysteresis loop in Fig. 1.

chosen such that $d_{33}E_0/\varepsilon_0 = 0.21$, selected to produce a shape comparable to experimental loops [1,30]. The origin is the starting point since the material is initially unpolarized. This also means that the material is not initially piezoelectric, as can be seen from Eq. (43). Thus no strain develops at first when the electric field is increased. However, polarization commences at $E = E_0$ and therefore the remanent strain grows quadratically with the polarization and piezoelectric strain appears and grows as well. The curve rises steeply at first because there is a rapid increase in polarization strain. However, lock up sets in and the slope of the curve diminishes. After the maximum field is reached and the then reduced, switching ceases and the response is at first purely linearly piezoelectric with the strain given by Eq. (43) with both ε^r and P^r non-zero and fixed. Therefore, the response to small electric fields at this stage is piezoelectric with a positive slope. As the field continues to be reduced, switching recommences at $E = -0.5E_0$ and since the remanent polarization is now diminishing, the remanent strain falls. Simultaneously, the piezoelectric effect is degraded and when the electric field reaches $-E_0$ and the remanent polarization is zero, the strain has reached zero as well. However, as the field is reduced below $-E_0$ a negative remanent polarization develops and the remanent and piezoelectric strains are rebuilt. Lock up now occurs as the electric field is brought towards $-1.5E_0$. After this value is reached, the electric field is

increased, switching is halted and the response is linear, given by Eq. (43) with ε^r and P^r both non-zero and fixed. However, the piezoelectric effect has now reversed so that when the field is brought back to zero, the response to small fields has a negative slope. The electric field is now increased again toward E_0. Switching recommences at $E = 0.5E_0$ to eliminate the existing negative remanent polarization. This is completed by the time the field reaches E_0 at which stage the strain once again goes to zero. As the field is cycled between $-1.5E_0$ and $1.5E_0$, the initial butterfly loop is repeated.

The stress–strain response of a poled material as shown in Fig. 3 is now computed as follows. The previous calculation yields a poled material after the field is increased to $1.5E_0$ and then reduced to zero. At this stage, the electric displacement (equal to the remanent polarization) is just below P_0 and the strain (purely remanent) is just below ε_0. A compressive stress is now applied and Eqs. (43) and (44) (with $E = 0$) are used to compute the strain, subject to Eqs. (34) and (40) if switching occurs. In these calculations, the same parameters are used as before but in addition, $Y/E_0P_0 = 100$. The initial response (at the right hand end of the plot in Fig. 3) is linear because Φ is less than zero and Eqs. (43) and (44) are used with P^r and therefore ε^r non-zero and fixed. However, as the compressive stress is increased, Φ eventually climbs up to zero and switching driven by the stress commences in such a way that the positive remanent polarization and remanent strain are reduced. During this process, Eq. (34) is used as the switching criterion with the

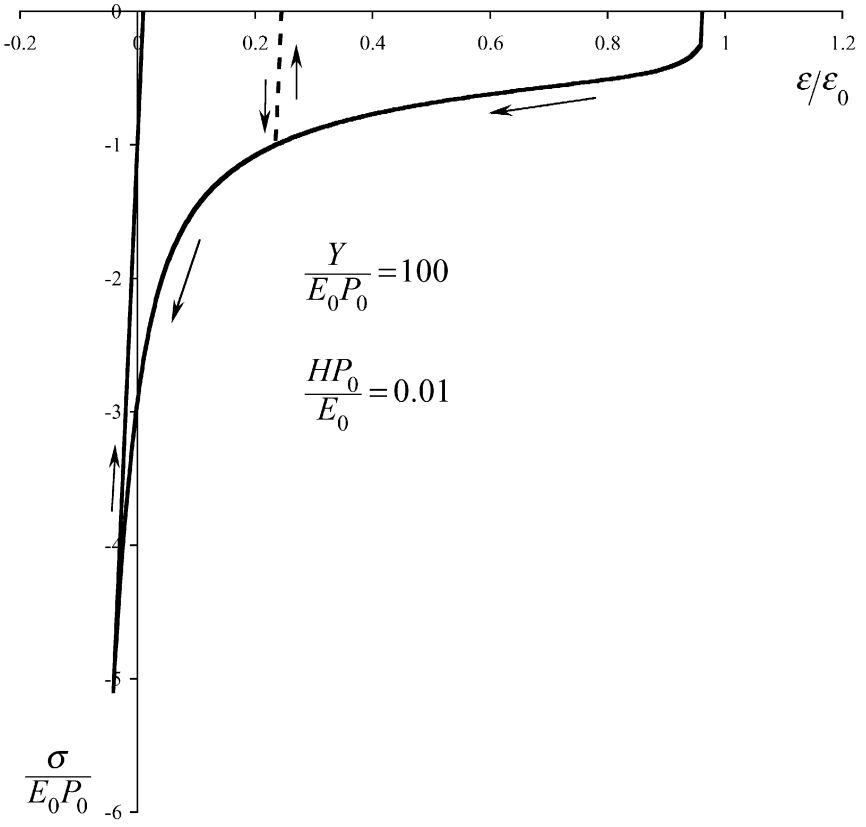

Fig. 3. Result from the constitutive law for a compressive stress–strain curve for a previously poled sample.

negative sign in the right hand side, the back electric field is computed from the remanent polarization from Eq. (40) and the remanent strain is computed from the remanent polarization from Eq. (44). The result is the non-linear response to be seen in Fig. 3 (moving from right to left as indicated by the arrows) in which the strain is decreasing while there is relatively little change in the stress. As the remanent polarization diminishes, the stress has less and less effect in terms of driving the switching, as can be deduced from Eq. (34). Therefore, the stress magnitude has to increase to keep the switching process going and the slope of the stress strain curve approaches elastic levels as the strain (and therefore the remanent polarization) is driven towards zero. After the stress has reached approximately $-5E_0P_0$, it is increased and switching stops because Φ falls below zero. The result is a linear response given by Eq. (43) with $E = 0$ and ε^r non-zero and fixed that prevails until the stress returns to zero. Afterwards, there is a relatively small positive remanent strain remaining. The residual remanent strain left after the stress falls to zero is positive because only positive remanent strains are permitted parallel to the remanent polarization in our model. This is a deficiency of the constitutive law that arises because we have chosen the remanent strain to be a unique function of the remanent polarization, whereas experimental data show that negative remanent strains are possible in a direction parallel to current or prior remanent polarizations. In particular, compressive stress applied parallel to the remanent polarization in experiments can produce negative remanent strains, in contrast to the results of our model shown in Fig. 3. Note that an intermediate unloading and reloading path has been shown in Fig. 3 in the form of a dashed line with arrows indicating the reversible path followed during this process.

The plot of stress versus electric displacement corresponding to Fig. 3 is shown in Fig. 4. The relevant equation from (7) that is needed for this is

$$D = \frac{P^r n}{P_0} d_{33}\sigma + \kappa E + P^r n \tag{45}$$

which is used in this case with $E = 0$. As with the stress–strain curve, the starting point on the curve is at the far right and one proceeds along the curve from right to left to follow the process as indicated by the arrows. This depolarization plot is very similar in form to the stress–strain curve, except that the change in linear response caused by the loss of the piezoelectric effect due to depolarization is quite noticeable. This feature can be seen clearly when the intermediate unloading/reloading path (dashed line) is compared with the final unloading path.

A series of hysteresis and butterfly loops are calculated now in which a compressive stress is applied and held fixed while the electric field is cycled. To obtain these loops, the material is first poled, i.e. an electric field of $1.5E_0$ is applied to an initially unpolarized material and the field is brought back to zero. The remanent polarization is then just below P_0 and the remanent strain is just below ε_0. The compressive stress is then applied and brought to the desired level. This is equivalent to starting at the right hand end of the stress–strain and depolarization plots in Figs. 3 and 4 and moving leftwards along them to a limited degree and stopping. With the compressive stress held fixed at the chosen level, an electric field is now introduced starting at zero and cycled between $-1.5E_0$ and $1.5E_0$ with the initial half cycle being positive. The electric displacement is calculated using Eq. (45) with Eqs. (34) and (40) utilized during switching. The strain is calculated using Eqs. (43) and (44). The same parameter values are used as were utilized in the earlier calculations.

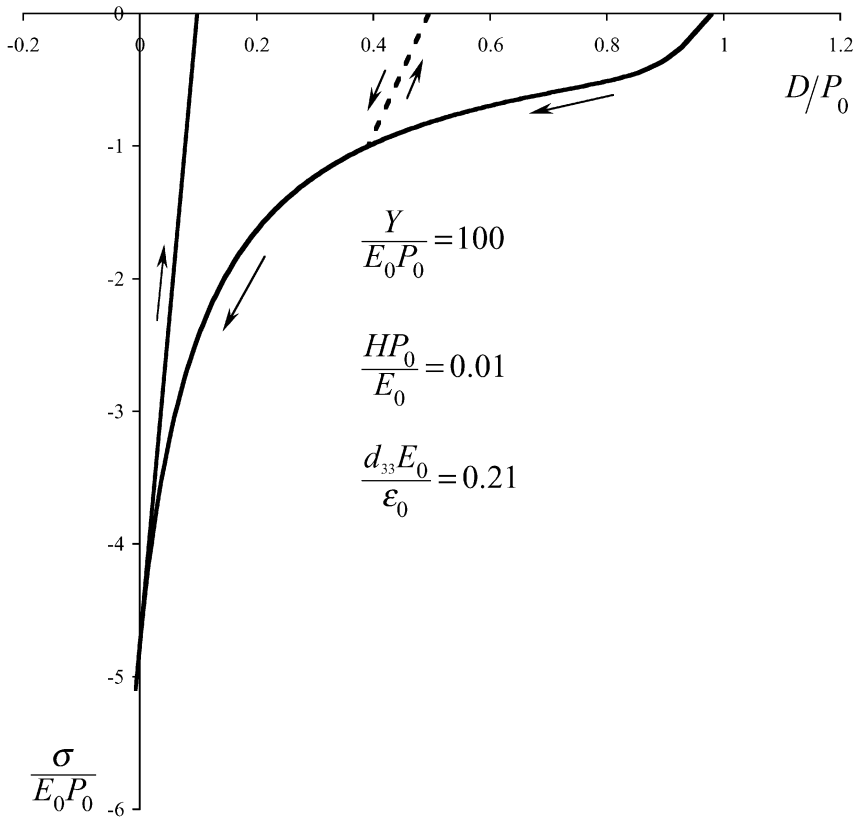

Fig. 4. Depolarization curve corresponding to the stress–strain curve in Fig. 3.

The hysteresis loops are shown in Fig. 5 and the butterfly loops are shown in Fig. 6. The initial response during the first half cycle of positive electric field is always linear and non-linear behavior commences only after the electric field becomes sufficiently negative. The compressive stress causes the hysteresis loops to rotate clockwise relative to that without stress. This is caused by the fact that the compressive stress clamps the remanent polarization and tends to eliminate it. Therefore, at a given level of remanent polarization, it takes a larger magnitude of electric field to cause switching to occur compared to when there is no compressive stress present. Consequently, the slope of the hysteresis curves during switching when a compressive stress is present is lower than when there is no compressive stress and the slope is inversely proportional to the compressive stress magnitude. Also, the extent of polarization achieved at the maximum magnitude of applied electric field is lessened in proportion to the applied stress. The resulting hysteresis loops are very similar to those measured experimentally and the trend relative to the application of greater amounts of compressive stress is quite realistic [30]. At higher compressive stresses, our computed loops are rather rectilinear unlike the measured ones which are more curvilinear [30]. However, this is caused by the function we use in Eq. (40) for E^{B} which is quite linear in appearance at lower values of remanent polarization. A more curvilinear function for E^{B} at lower magnitudes of

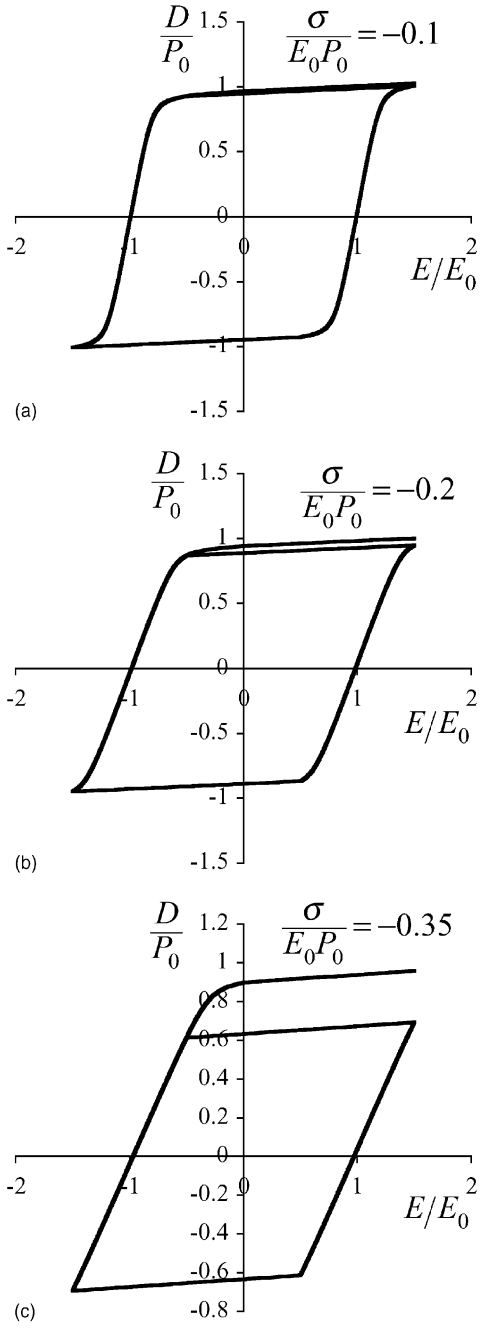

Fig. 5. Result from the constitutive law for hysteresis loops for a previously poled material subject to a fixed compressive stress during cycling of the electric field: a–c are for ascending levels of compressive stress.

remanent polarization would produce more curvilinear hysteresis loops when significant compressive stress is applied.

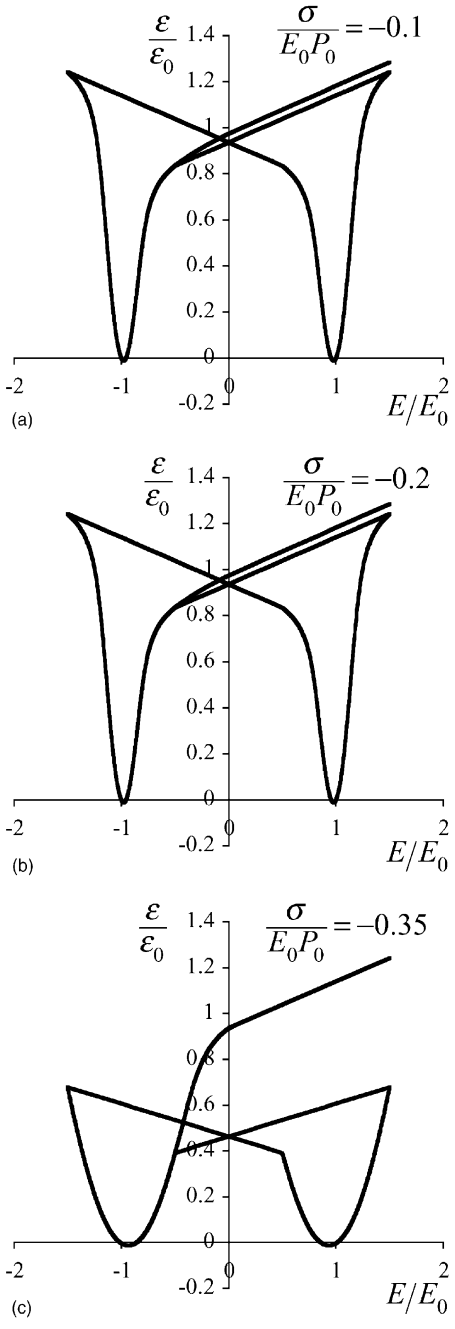

Fig. 6. Butterfly loops corresponding to the hysteresis loops in Fig. 5.

The butterfly loops shown in Fig. 6 illustrate the same effects that are visible in the hysteresis loops. The clamping effect of the compressive stress diminishes the remanent strain at fixed levels

of electric field. As a result the butterfly loops move downwards on the strain axis as the compressive stress is increased and the tails of the butterflies are broadened. In addition, because the remanent polarization is diminished by the clamping effect of the compressive stress, the effective piezoelectric coefficient is lessened. As is the case with the hysteresis loops, the butterfly loops obtained subject to a compressive stress have a realistic appearance compared to experimental ones, including the trend as the compressive stress is increased [30]. It should be noted that it is possible to produce loops equivalent to those in Figs. 5 and 6, but with a higher compressive stress applied. We have calculated and studied such loops but we decline to illustrate them in this paper. They appear qualitatively to be quite satisfactory in comparison with the experimental loops in [30]. However, quantitatively these loops are not satisfactory because the remanent strain does not diminish sufficiently as the compressive stress is increased and does not become negative at the highest compressive stresses. This is related to the deficiency of our model that we addressed in the context of Fig. 3 and is tied directly to the fact that we have made the remanent strain uniquely dependent on the remanent polarization.

Calculations are also carried out for polarization rotation as occurs in experiments of Huber and Fleck [2]. In these experiments, a plate of PZT was first poled and the electrodes etched away. Then, specimens were cut from the poled plate and new electrodes applied to them so that an electric field could be imposed at an angle relative to the pre-existing polarization. As the electric field is increased, the remanent polarization rotates so that the angle between the polarization direction and the electric field reduces. In cases where the angle is initially obtuse, depolarization may first occur followed by repolarization parallel to the electric field. The constitutive law was used to simulate these experiments. The experiments are carried out without stress being applied, and so the form of the constitutive law that is purely electrical can be used to model them. In this case, the switching criterion becomes

$$\Phi = (E_i - E_i^{\mathrm{B}})(E_i - E_i^{\mathrm{B}}) - E_0^2 = 0 \tag{46}$$

and the switching rate law is

$$\dot{P}_i^{\mathrm{r}} = \frac{(E_i - E_i^{\mathrm{B}})(E_j - E_j^{\mathrm{B}})\dot{E}_j}{(E_i - E_i^{\mathrm{B}})H_{ij}(E_j - E_j^{\mathrm{B}})} \tag{47}$$

The results of the simulation are shown in Fig. 7, which shows the change of the component of the electric displacement parallel to the direction of the applied electric field as a function of the applied electric field. In these calculations, the same set of constitutive parameters utilized above has been used. A series of curves is shown each with a different angle initially between the remanent polarization and the electric field vectors. In each case, the increment ΔD of the electric displacement is the change from the state at zero electric field. Clearly, the curve for an initial angle of 180° is a half hysteresis loop whereas the response when the angle is initially zero is nearly linear. The latter case arises because the material is approaching lock up and the electric field is simply driving it further into this state. For angles in between, the behavior involves a gradual transition from the half hysteresis loop for an initial angle of 180° to linear behavior when the angle is zero. This is exactly what happens in the experiments [2].

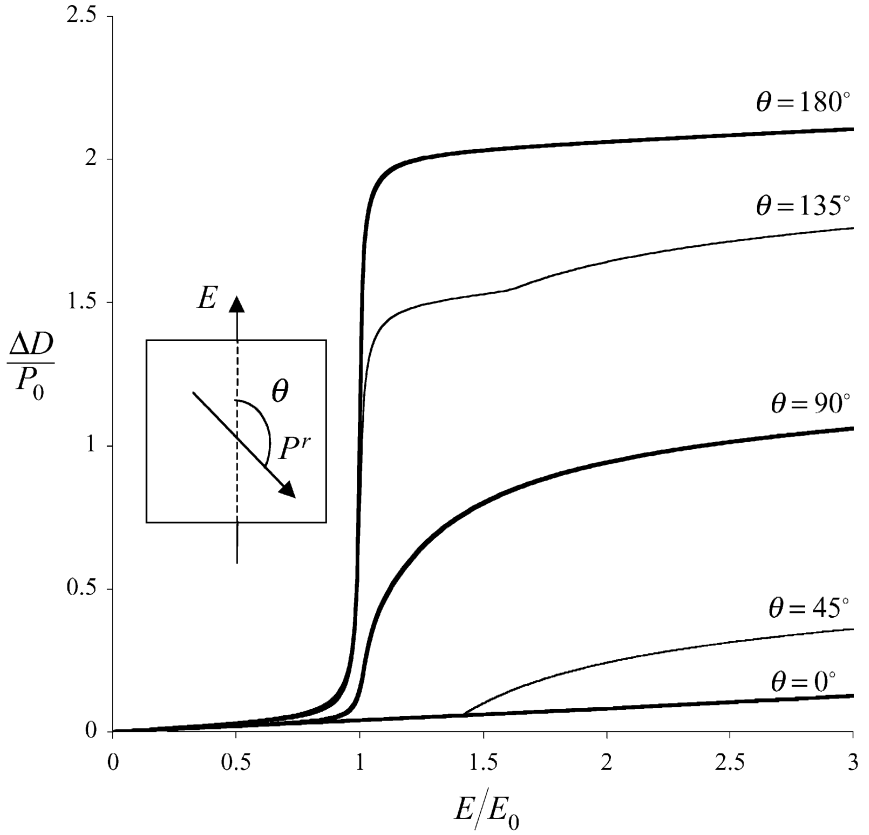

Fig. 7. Polarization rotation curves obtained from the constitutive law. The component of the electric displacement parallel to the applied electric field is plotted against the electric field.

Plots of the strain are given in Fig. 8, corresponding to the results in Fig. 7. In addition to using $d_{15} = d_{33} - d_{31}$, the quantity d_{31} was taken to be equal to $-d_{33}/2$ for these calculations. The datum for the strain is the beginning of the experiment when the electric field is first applied. It can be seen that the curve for an initial angle of 180° is a half butterfly loop, showing that as the polarization reverses, the material first contracts as the polarization disappears and then the specimen extends when the polarization is rebuilt. A linear response is obtained for an initial angle of zero. This behavior is simply the nearly linear (i.e. piezoelectric) response of a material that is already locked up. Note the interesting feature that the final strains in these two cases converge as the electric field is increased. This is because the final state of polarization is the same in both cases but in the beginning was opposite. The quadratic dependence of strain on polarization means that both the initial and final strains are the same for these two situations. In the case of an initial angle of 90°, there is no strain response to begin with. This occurs because the electric field is orthogonal to the initial polarization, meaning that there is no piezoelectric response at the beginning in the direction of the applied field. Eventually polarization rotation commences and then the polarization strain appears accompanied by some piezoelectric response. In the case of an initial angle of 135°, the response is similar to the that for 180°, except that there is less loss of strain to begin

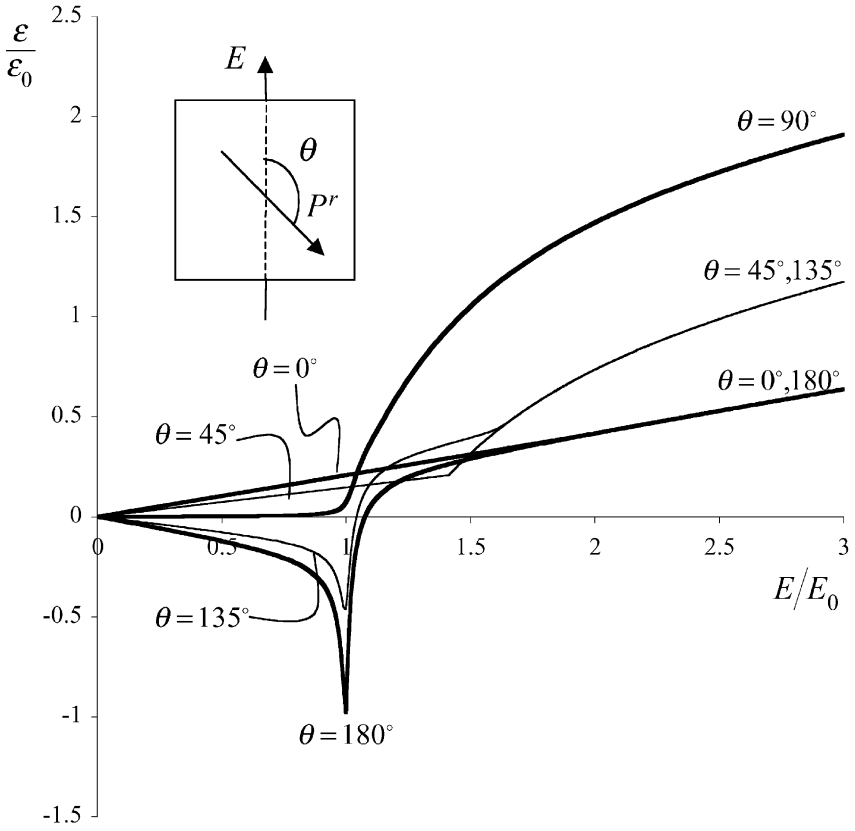

Fig. 8. Strain versus electric field curves corresponding to the polarization rotation plots in Fig. 7.

with and a greater accumulation of strain at the end. The case of an initial angle of 45° responds at first like the zero angle situation but with a lower piezoelectric coefficient. Eventually, polarization rotation occurs in the 45° case and then the strain rises above that of the zero angle example. As the electric field is increased, the strain for the cases with initial angles 45° and 135° converge. This occurs for similar reasons to the parallel and anti-parallel cases. The initial strain in the direction of the applied electric field is the same for the two cases despite the difference in orientation of the initial polarization. The final strain is the same because the final state of polarization is identical in the two situations.

6. Discussion

The proposed constitutive law has been used to compute a series of hysteresis and butterfly loops, a stress–strain, a stress-depolarization curve and to simulate polarization rotation. Other than the fact that our remanent strain parallel to the remanent polarization is always positive, the features of these loops and curves reproduce the qualitative behavior observed in experimentally

measured results for polycrystalline ferroelectric ceramics. All the available data on constitutive behavior of ferroelectrics has been modeled in these loops and curves.

The primary shortcoming of the proposed constitutive model is that it is not able to produce compressive strains parallel to the polarization direction. Furthermore, in the absence of polarization the model cannot produce remanent strain at all. These features are in contradiction to experimental measurements on real ferroelectric materials. Measurements performed in [30] have demonstrated that even in the absence of remanent polarization, the application of stress can cause the material to strain irreversibly. Depolarization experiments performed in [30] have also demonstrated that while compressive stress does depole a polarized sample, some remanent polarization remains even when the material is forced into a significantly compressive remanent strain state. Hence, we must conclude that the remanent strain and the remanent polarization in ferroelectric material are generally decoupled and Eq. (12) does not capture all of the physics of the deformation and polarization processes.

However, it is likely that the model presented in this paper is useful for obtaining qualitative predictions about structures made of ferroelectric materials. In fact, we would argue that the model performs adequately when the applied stresses are relatively small compared to the applied electric fields. With the overall qualitative nature of the model in mind, Eq. (12) presents a significant simplification over more general constitutive models like that found in [29]. The benefits of the model include simplicity of implementation within a finite element framework [34] and the likelihood that it can provide qualitative insights into the design of sensing and actuating structures. On the first point, Landis has recently developed a finite element method for electromechanical problems using a vector potential that generates the electric displacement as the independent nodal variable for the electrical part of the problem. As a consequence, in this finite element method the electric displacement and the strain are equivalent degrees of freedom within elements and stress and electric field are equivalent conjugate variables. Therefore, the constitutive law formulation presented here and also that used by Landis [29] fits naturally into the new finite element method presented in Ref. [34]. On the second point, Haug and McMeeking, in unpublished work, have already used the constitutive framework presented here to model the poling of a stack actuator.

Acknowledgements

The authors wish to thank Albrecht Liskowsky of the Technische Universität Dresden for assistance computing and plotting loops and curves. This research was carried out with support from the National Science Foundation through Grant CMS-9813022.

References

[1] B. Jaffe, W.R. Cook, H. Jaffe, Piezoelectric Ceramics, Academic Press, London and New York, 1971.
[2] J.E. Huber, N.A. Fleck, Multi-axial electrical switching of a ferroelectric: theory versus experiment, Journal of the Mechanics and Physics of Solids 49 (2001) 785–811.
[3] T. Steinkopff, Finite-element modelling of ferroelectric domain switching in piezoelectric ceramics, Journal of the European Ceramic Society 19 (1999) 1247–1249.

[4] K. Chan, N. Hagood, Modeling of nonlinear piezoceramics for structural actuation, Proceedings of SPIE Symposium on Smart Structures and Materials 2190 (1994) 194–205.
[5] S.C. Hwang, C.S. Lynch, R.M. McMeeking, Ferroelectric/ferroelastic interactions and a polarization switching model, Acta Metallurgica et Materialia 43 (1995) 2073–2084.
[6] S.C. Hwang, J.E. Huber, R.M. McMeeking, N.A. Fleck, The simulation of switching in polycrystalline ferroelectric ceramics, Journal of Applied Physics 84 (1998) 1530–1540.
[7] W. Chen, C.S. Lynch, A micro-electro-mechanical model for polarization switching of ferroelectric materials, Acta Materialia 46 (1998) 5303–5311.
[8] W. Chen, C.S. Lynch, Finite element analysis of cracks in ferroelectric ceramic materials, Engineering Fracture Mechanics 64 (1999) 539–562.
[9] J.E. Huber, N.A. Fleck, C.M. Landis, R.M. McMeeking, A constitutive model for ferroelectric polycrystals, Journal of the Mechanics and Physics of Solids 47 (1999) 1663–1697.
[10] X. Chen, D.N. Fang, K.C. Hwang, Micromechanics simulation of ferroelectric polarization switching, Acta Materialia 45 (1997) 3181–3189.
[11] P.J. Chen, P.S. Peercy, One dimensional dynamic electromechanical constitutive relations of ferroelectric materials, Acta Mechanica 31 (1979) 231–241.
[12] P.J. Chen, S.T. Montgomery, A macroscopic theory for the existence of the hysteresis and butterfly loops in ferroelectricity, Ferroelectrics 23 (1980) 199–208.
[13] P.J. Chen, Three dimensional dynamic electromechanical constitutive relations for ferroelectric materials, International Journal of Solids and Structures 16 (1980) 1059–1067.
[14] P.J. Chen, M.M. Madsen, One dimensional polar response of the electrooptic PLZT 7/65/35 due to domain switching, Acta Mechanica 41 (1981) 255–264.
[15] X. Zhou, A. Chattopadhyay, Hysteresis behavior and modeling of piezoceramic actuators, Journal of Applied Mechanics 68 (2001) 270–277.
[16] E. Bassiouny, A.F. Ghaleb, G. Maugin, Thermodynamical formulation for coupled electromechanical hysteresis effects-I Basic equations, International Journal of Engineering Science 26 (1988) 1279–1295.
[17] E. Bassiouny, A.F. Ghaleb, G. Maugin, Thermodynamical formulation for coupled electromechanical hysteresis effects-II Poling of ceramics, International Journal of Engineering Science 26 (1988) 1297–1306.
[18] E. Bassiouny, G. Maugin, Thermodynamical formulation for coupled electromechanical hysteresis effects-III Parameter identification, International Journal of Engineering Science 27 (1989) 975–987.
[19] E. Bassiouny, G. Maugin, Thermodynamical formulation for coupled electromechanical hysteresis effects-IV Combined electromechanical loading, International Journal of Engineering Science 27 (1989) 989–1000.
[20] M. Kamlah, C. Tsakmakis, Phenomenological modeling of the non-linear electromechanical coupling in ferroelectrics, International Journal of Solids and Structures 36 (1999) 669–695.
[21] M. Kamlah, U. Böhle, D. Munz, C. Tsakmakis, Macroscopic description of the non-linear electro-mechanical coupling in ferroelectrics, in: V.V. Varadan, J. Chandra (Eds.), Smart Structures and Materials 1997: Mathematics and Control in Smart Structures, Proceedings of SPIE 3039 (1997) 144–155.
[22] M. Kamlah, U. Böhle, On a non-linear finite element method for piezoelectric structures made of hysteretic ferroelectric ceramics, in: C.S. Lynch (Ed.), Smart Structures and Materials 2000: Active Materials: Behavior and Mechanics, Proceedings of SPIE 3992 (2000) 255.
[23] M. Kamlah, U. Böhle, Finite element analysis of piezoceramic components taking into account ferroelectric hysteresis behavior, International Journal of Solids and Structures 38 (2001) 605–633.
[24] M. Kamlah, U. Böhle, D. Munz, On a non-linear finite element method for piezoelectric structures made of hysteretic ferroelectric ceramics, Computational Materials Science 19 (2000) 81–86.
[25] M. Kamlah, Ferroelectric and ferroelastic piezoceramics—modeling of electromechanical hysteresis phenomena, Continuum Mechanics and Thermodynamics 13 (2001) 219–268.
[26] U. Böhle, Phänomenologische Modellierung und Finite-Elemente-Simulationen von nichtlinearen elektromechanischen Vorgängen in ferroelektrischen Materialen, Forschungszentrum Karlsruhe Wissenschaftliche Bericht FZKA 6347, 1999.
[27] A.C.F. Cocks, R.M. McMeeking, A phenomenological constitutive law for the behavior of ferroelectric ceramics, Ferroelectrics 228 (1999) 219–228.

[28] R.M. McMeeking, Phenomenological constitutive models for ferroelectric ceramics, Abstract and presentation, SPIE Smart Structures and Materials 2000 Conference: Active Materials: Behavior and Mechanics, Newport Beach, CA, March 6–9, 2000.
[29] C.M. Landis, Fully coupled, multi-axial, symmetric constitutive laws for polycrystalline ferroelectric ceramics, Journal of the Mechanics and Physics of Solids 50 (2002) 127–152.
[30] C.S. Lynch, The effect of uniaxial stress on the electro-mechanical response of 8/65/35 PLZT, Acta Materialia 44 (1996) 4137–4148.
[31] D. Berlincourt, H. Jaffe, Elastic and piezoelectric coefficients of single crystal barium titanate, Physical Review 111 (1958) 143–148.
[32] R. Hill, The Mathematical Theory of Plasticity, Oxford University Press, 1950.
[33] A. Haug, V. Knoblauch and R.M. McMeeking, Combined isotropic and kinematic hardening in phenomenological switching models for ferroelectric ceramics, submitted for publication.
[34] C.M. Landis, A new finite element formulation for electromechanical boundary value problems, International Journal for Numerical Methods in Engineering 55 (2002) 613–628.